Neuron to glia signaling triggers myelin membrane exocytosis from endosomal storage sites

Katarina Trajkovic,[1,2] Ajit Singh Dhaunchak,[2] José T. Goncalves,[2] Dirk Wenzel,[1] Anja Schneider,[1,2] Gertrude Bunt,[2] Klaus-Armin Nave,[2] and Mikael Simons[1,2]

[1]Centre for Biochemistry and Molecular Cell Biology, University of Göttingen, 37073 Göttingen, Germany
[2]Max-Planck-Institute for Experimental Medicine, 37075 Göttingen, Germany

During vertebrate brain development, axons are enwrapped by myelin, an insulating membrane produced by oligodendrocytes. Neuron-derived signaling molecules are temporally and spatially required to coordinate oligodendrocyte differentiation. In this study, we show that neurons regulate myelin membrane trafficking in oligodendrocytes. In the absence of neurons, the major myelin membrane protein, the proteolipid protein (PLP), is internalized and stored in late endosomes/lysosomes (LEs/Ls) by a cholesterol-dependent and clathrin-independent endocytosis pathway that requires actin and the RhoA guanosine triphosphatase. Upon maturation, the rate of endocytosis is reduced, and a cAMP-dependent neuronal signal triggers the transport of PLP from LEs/Ls to the plasma membrane. These findings reveal a fundamental and novel role of LEs/Ls in oligodendrocytes: to store and release PLP in a regulated fashion. The release of myelin membrane from LEs/Ls by neuronal signals may represent a mechanism to control myelin membrane growth.

Introduction

The myelin sheath is a multilamellar, spirally wrapping extension of the plasma membrane of oligodendrocytes that is essential for rapid impulse conduction in the central nervous system. This specialized membrane exhibits a unique composition with >70% of the dry weight consisting of lipids and the remainder being comprised of a restricted set of proteins, of which most are exclusively found in myelin (Baumann and Pham-Dinh, 2001; Kramer et al., 2001). The major central nervous system myelin proteins, the myelin basic protein, and the proteolipid proteins (PLPs/DM20) are low molecular weight proteins found in compact myelin that constitute 80% of the total myelin proteins. PLP is a highly hydrophobic protein with four transmembrane domains that interact with cholesterol and galactosylceramide-enriched membranes during its biosynthetic transport in oligodendrocytes (Weimbs and Stoffel, 1992; Simons et al., 2000; Schneider et al., 2005).

To form the myelin sheath, oligodendrocytes must deliver large amounts of myelin membrane to the axons at the appropriate developmental stage of the oligodendroglial and neuronal

cell lineage (Baumann and Pham-Dinh, 2001; Kramer et al., 2001). On the other hand, axons produce signals that regulate the differentiation of oligodendrocytes (Barres and Raff, 1999; Fields and Stevens-Graham, 2002). This led us to postulate that neuronal signals could be involved in the coordination of the trafficking of myelin membrane in oligodendrocytes. In this study, we show that the transport of PLP in oligodendrocytes is under neuronal control. PLP is initially targeted to late endosomes/lysosomes (LEs/Ls) by using a cholesterol-dependent and clathrin-independent endocytosis pathway. PLP is then redistributed from LEs/Ls to the plasma membrane upon activation by neuronal cells. We provide evidence that this development-dependent regulation of PLP localization occurs by the down-regulation of endocytosis and by the stimulation of exocytosis from LE/L storage sites.

Results

PLP localizes to LEs/Ls of immature oligodendrocytes

To analyze the localization of PLP in immature oligodendrocytes, oligodendroglial precursor cells growing on top of a layer of astrocytes were shaken off and cultured for 3 d to induce the expression of PLP. By confocal immunofluorescence microscopy, extensive colocalization of PLP and Lamp-1, a marker for
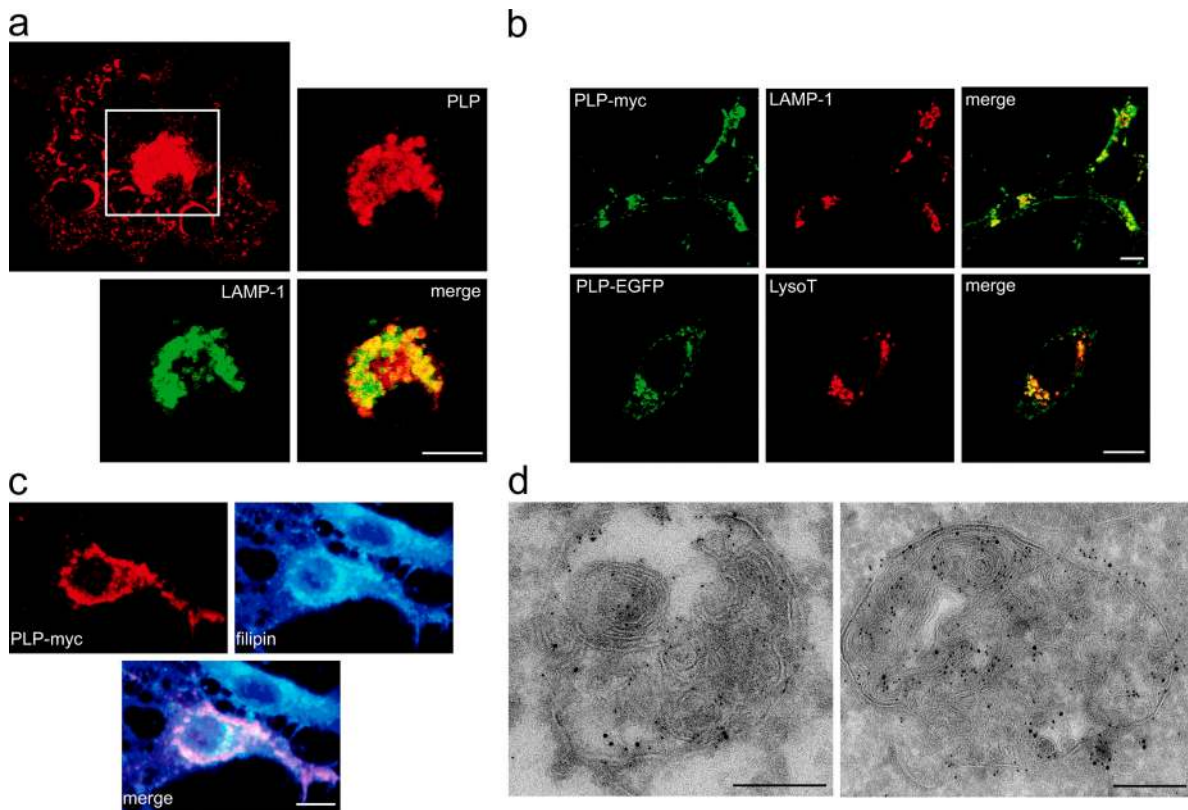
Figure 1. **PLP localizes to LEs/Ls of immature oligodendrocytes.** (a) Confocal immunofluorescence microscopy demonstrates the colocalization of endogenous PLP (red) with Lamp-1 (green) in primary oligodendrocytes grown for 3 d in vitro. The region in the boxed area is shown at higher magnification and lower exposure. (b) Top panels show the colocalization of PLP-myc (green) with Lamp-1 (red) in Oli-neu cells, and the bottom panels show the colocalization of PLP-EGFP (green) with LysoTracker red in living OLN-93 cells. (c) Filipin staining reveals colocalization of cholesterol (blue) and PLP (red) in OLN-93 cells. (a–c) Bars, 5 μm. (d) Immuno-EM double labeling of primary oligodendrocytes (left) and Oli-neu cells (right) with antibodies directed against Lamp-1 (5 nm gold) and against PLP, polyclonal P6 (left), or GFP (right; both 10 nm gold) shows the localization of PLP in Lamp-1–containing multivesicular and multilamellar compartments. Bars, 200 nm.

LEs/Ls, was observed (Fig. 1 a) as reported previously (Kramer et al., 2001; Simons et al., 2002). The same striking colocalization of PLP and Lamp-1 was observed in an immortalized oligodendroglial precursor cell line, Oli-neu. Fusion of either a myc tag or EGFP to PLP did not affect the LE/L targeting of PLP (Fig. 1 b). To obtain further support for the localization of PLP to LEs/Ls in immature cells, we used a spontaneously transformed oligodendroglial precursor cell line, OLN-93. When these cells were incubated for 5 h with rhodamine–dextran followed by a 2-h chase or were treated with LysoTracker red DND-99 to stain for LEs/Ls, colocalization with PLP was observed (Fig. 1 b and not depicted). Staining with filipin revealed a partial colocalization of PLP with cholesterol in LEs/Ls (Fig. 1 c).

To resolve the ultrastructure of the PLP-containing organelles, we performed immunoelectron microscopy (Fig. 1 d). Both endogenous PLP and PLP-EGFP colocalized with Lamp-1 in vacuolar structures that contained abundant lumenal multilamellar and/or multivesicular membrane arrays.

PLP disappears from LEs/Ls when oligodendrocytes are cocultured with neurons

To determine whether the subcellular localization of PLP is influenced by the presence of neuronal cells, oligodendroglial progenitor cells were added to a neuronal cell culture. Similar to the cultures without neurons, oligodendrocytes started to

Figure 2. **PLP disappears from LEs/Ls when oligodendrocytes are cocultured with neurons.** (a) Primary oligodendrocytes were grown for 3 or 5 d with or without neurons. Confocal microscopy analysis of PLP (red) and Lamp-1 (green) demonstrates a depletion of PLP from LEs/Ls in oligodendrocytes when cultured in the presence of neurons for 5 d. Axons are visualized by βIII-tubulin staining (blue). (b) Oli-neu cells were grown for 2 d with (bottom) or without (top) neurons. PLP-EGFP (green) disappears from Lamp-1–containing compartments (red) by 2 d of coculture with neurons. (a and b) The regions in the boxed areas are shown at a higher magnification and lower exposure. (c) Surface staining of living cells with O10 mAb at 4°C shows that the majority of PLP-EGFP is found at the surface of the cell in a coculturing with neurons. Quantitative analysis of the colocalization of PLP-EGFP with Lamp-1 (b) and O10 (c) are shown. Error bars represent SD ($n > 30$ cells). (a–c) Bars, 5 μm. (d) Immunohistochemistry of brain sections of P7 and P60 adult mice for PLP (red) and Lamp-1 (green). Colocalization was observed in sections from P7 but not adult mice. Bars, 10 μm. (e) Oligodendrocytes (for 2 d in culture) grown with or without neurons were metabolically labeled with [^{35}S]methionine/cysteine for 18 h and chased for 2 d (day 5) or not chased (day 3) before performing the PLP immunoprecipitations. Quantitative analysis of three independent experiments did not reveal any significant differences in the amount of labeled PLP and its alternatively spliced isoform DM20 (mean ± SD). **, $P < 0.001$; t test.
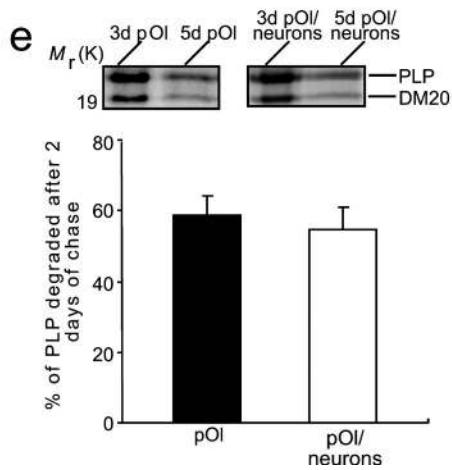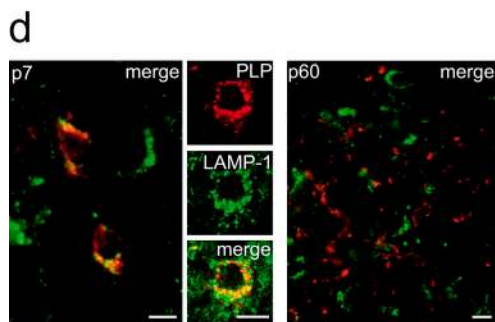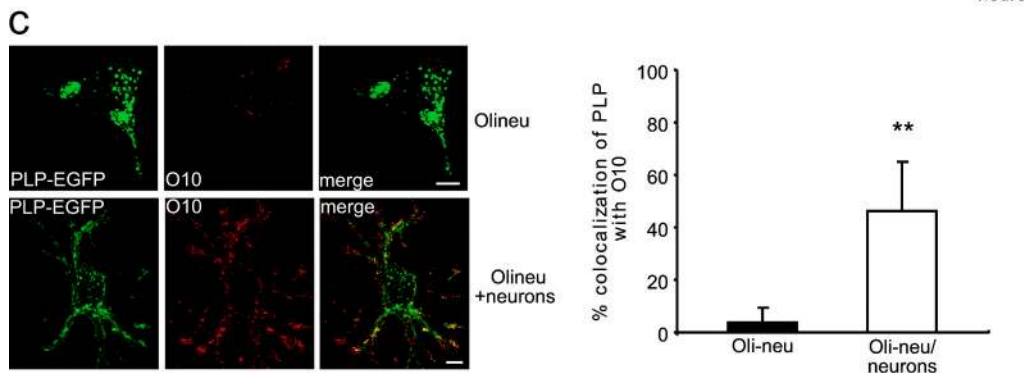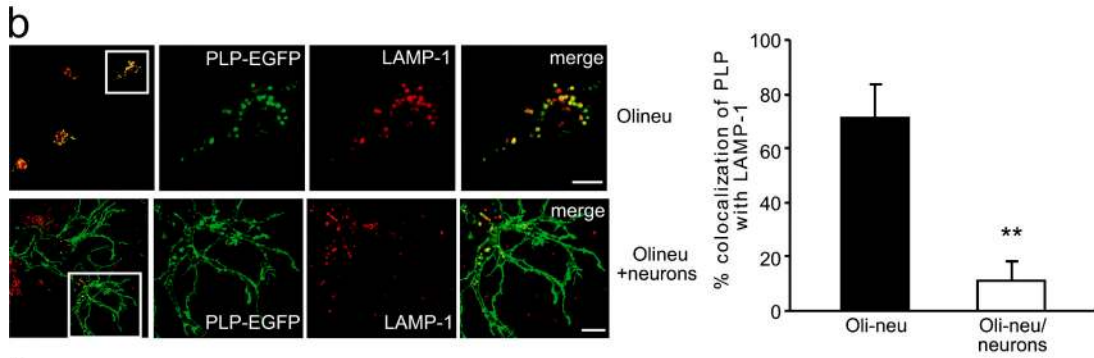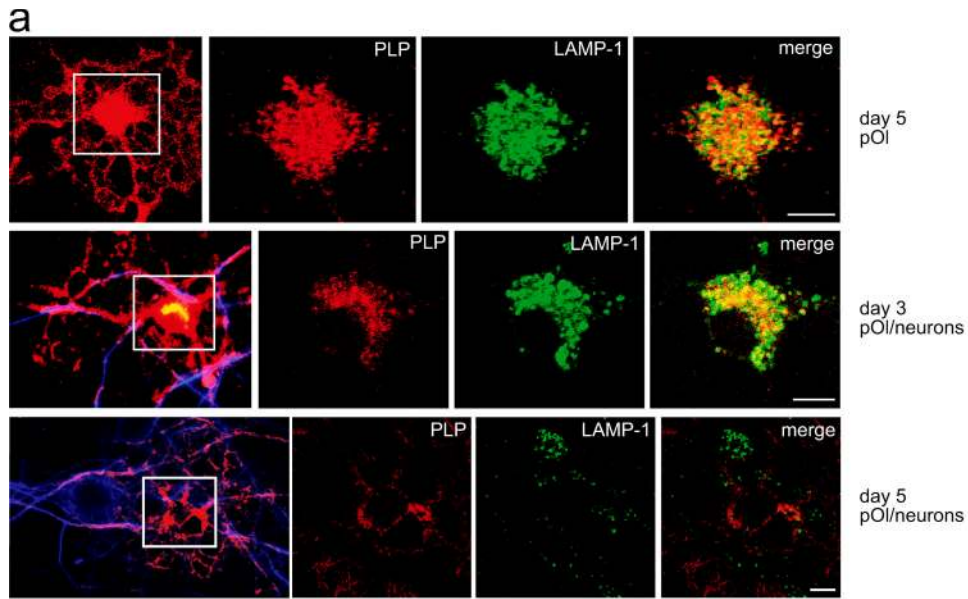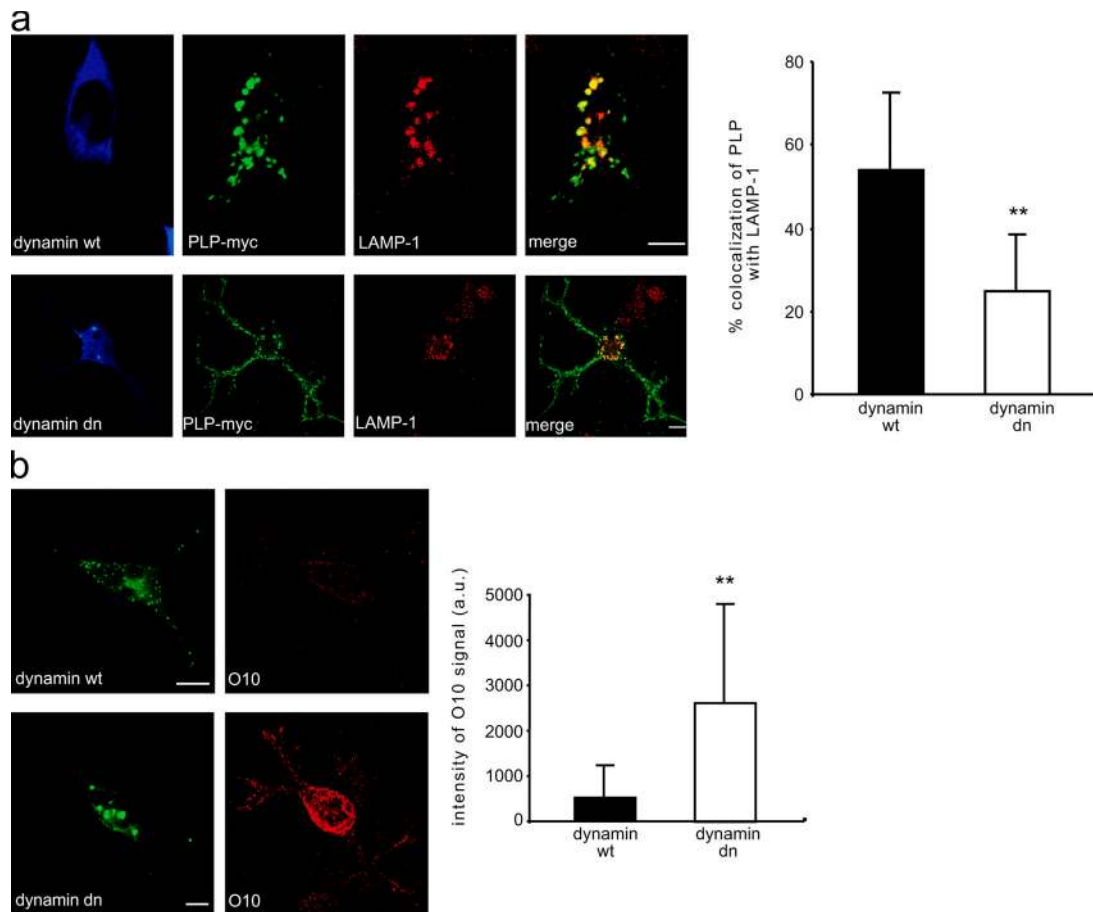
Figure 3. **PLP is routed to LEs/Ls by endocytosis.** Oli-neu cells were cotransfected with PLP-myc and wild-type or dominant-negative dynamin-II (K44A, dynamin dn), both containing an HA tag, and were stained for Lamp-1 (a) or for surface PLP (b) with O10 mAb (at 4°C on living cells). (a) Quantitative analysis of the colocalization of PLP-EGFP with Lamp-1 is shown. (b) Quantitative analysis of the fluorescence intensity of O10 signal is shown in arbitrary units (a.u.) per cell. (a and b) Values are given as the means ± SD (error bars) of a mean of three independent experiments with >40 (a) or >30 (b) cells. **, P < 0.001; t test. Bars, 5 μm.

express PLP during the first 2 d in culture, and an accumulation of PLP in LEs/Ls was observed in ~90% of the cells after 3 d in culture (Fig. 2 a). However, in marked contrast to cultures without neurons, we observed that PLP disappeared from LEs/Ls 2 d later (only ~20% of the cells showed an accumulation of PLP in LEs/Ls) in the presence of neurons (Fig. 2 a). Also, the staining of Lamp-1–containing structures decreased in intensity after PLP removal. To follow the developmental regulation of PLP trafficking in Oli-neu cells, we produced PLP-EGFP–stably expressing cell lines. Fusion of EGFP to PLP did not interfere with transport to the cell surface, as indicated by the positive staining of transfected Oli-neu cells with O10 mAb. This antibody recognizes a conformation-dependent epitope of PLP on the surface of living cells (Jung et al., 1996). In addition, transfection of primary myelinating oligodendrocytes confirmed that PLP-EGFP is transported to myelin (Fig. S1, available at http://www.jcb.org/cgi/content/full/jcb.200509022/DC1). When PLP-EGFP–expressing Oli-neu cells were added on top of a neuronal culture, a dramatic change in the localization of PLP was observed (Fig. 2 b). Quantitative analysis showed that 71.5% of PLP colocalized with Lamp-1 in Oli-neu cells alone, whereas only 11.5% of PLP colocalized with Lamp-1 in

cells that had been in coculture with neurons for 2 d (Fig. 2 b). Moreover, surface staining of living cells at 4°C with O10 mAb showed that the majority of PLP-EGFP was located at the plasma membrane in cells cultured with but not without neurons (Fig. 2 c). To test whether the localization of PLP shows the same developmental regulation in vivo, we performed immunohistochemistry on brain sections of young (postnatal day [P] 7) and adult mice (P60). Significant colocalization of PLP and Lamp-1 was only observed in cells of P7 mice but not in sections prepared from adult mice (Fig. 2 d). Analysis of the sections indicated that the colocalization of PLP and Lamp-1 was increased >20-fold in P7 mice as compared with adult mice. Together, our data demonstrate that PLP disappears from LEs/Ls upon oligodendroglial maturation and emerges at the surface of the oligodendrocyte in a process that is dependent on the presence of neuronal cells.

There are several possibilities to explain our results. One possibility is that less PLP is transported into and/or more PLP is transported out of LEs/Ls in the presence of neurons. An alternative explanation is that the degradation of PLP in lysosomes increases during development. To test the latter hypothesis, we performed pulse-chase experiments. Primary oligodendrocytes
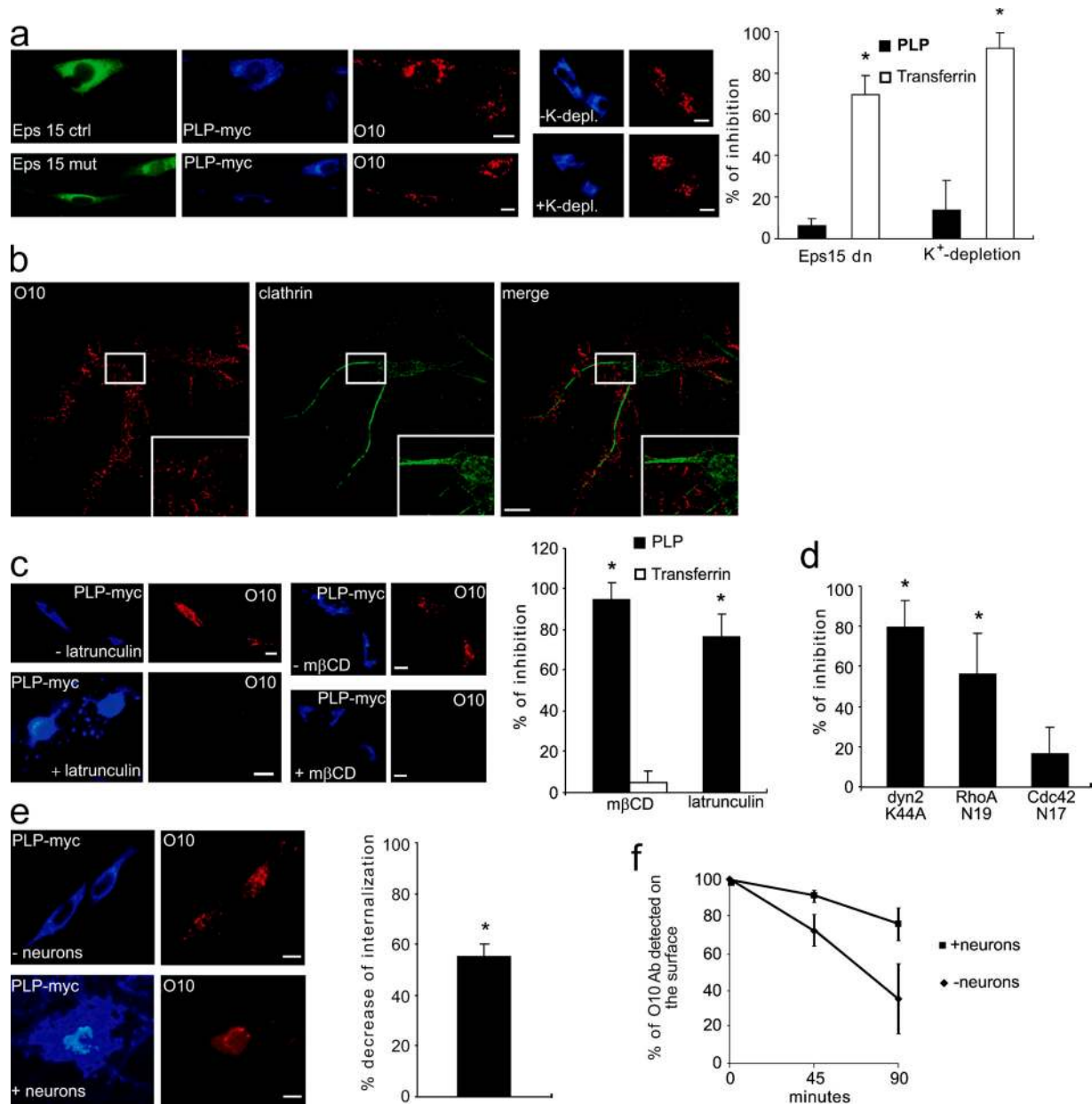
Figure 4. **The cholesterol-dependent and clathrin-independent internalization of PLP is reduced after coculturing with neurons.** Antibody uptake experiments were performed with the PLP antibody O10 followed by an acidic wash to remove surface-bound antibody. The internalized antibody is shown in red. (a) OLN-93 cells were cotransfected with PLP (blue) and with Eps15IIIΔ2 (Eps15 ctrl) or Eps15 EΔ95/295 (Eps15 mut; green). Potassium depletion was used as an alternative approach to interfere with clathrin function. Clathrin-mediated transferrin–rhodamine uptake served as a control. The amount of inhibition was evaluated by determining the fluorescence intensities in comparison with the control conditions. Values are given as the mean ± SD (error bars) of a mean of three independent experiments with >50 cells. (b) PLP stained with O10 (red) on the surface of OLN-93 cells does not show a significant colocalization with clathrin heavy chain (green). Insets are shown at higher magnification in the right corner of the images. (c) OLN-93 cells were transfected with PLP (blue) followed by a 30-min treatment with 1 μM latrunculin to inhibit the polymerization of the actin cytoskeleton or by a 15-min incubation with 5 mM mβCD to deplete cholesterol before performing the O10 internalization assay. Transferrin–rhodamine was used as a control for the cholesterol depletion experiments. Inhibition of the O10 uptake is shown as the mean ± SD of three independent experiments with >50 cells. (d) Cells were cotransfected with PLP and with wild type or the respective dominant-negative variants of dynamin-II, RhoA, and cdc42. The inhibition of O10 antibody uptake by the dominant-negative protein is shown in comparison with the respective wild-type construct as the mean ± SD of three independent experiments with >40 cells. The inhibition of fluid phase endocytosis (measured by dextran uptake) served as a positive control for dominant-negative cdc42 (not depicted). (e) OLN-93 cells were transfected with PLP-myc and added on top of a neuronal culture or left alone. O10 antibody uptake experiments were performed followed by an acidic wash to remove surface-bound antibody. The amount of inhibition is shown for OLN-93 cells cultured with neurons compared with cells cultured without neurons as the mean ± SD of three experiments with >40 cells. (f) The reduction of cell surface PLP was determined after various times in culture with or without neurons. Cell surface PLP was labeled with O10 mAb at 4°C, and incubation was continued at 37°C for 0, 45, and 90 min. The amount of cell surface remaining O10 mAb was analyzed by incubating cells with [125I]-labeled secondary antibody at 4°C and subsequent determination of the radioactivity by γ counting. Quantification is shown as the mean ± SD of three experiments. *, P < 0.01; t test. Bars, 5 μm.

(for 2 d in culture) grown with or without neurons were metabolically labeled with [^{35}S]methionine/cysteine for 18 h and chased for 2 d. Hence, the metabolic labeling was performed at the stage of development (day 2–3) when PLP accumulates in LEs/Ls. The cells were chased up to the developmental stage (day 5) when PLP is almost completely removed from LEs/Ls in cells cultured with neurons but not in cells cultured without. Nevertheless, we did not observe any significant differences in the amount of labeled PLP and its alternatively spliced isoform DM20 (Fig. 2 e). Thus, differential proteolysis of PLP does not seem to be the underlying reason for the removal of PLP from LEs/Ls. Therefore, it is more likely that neuronal signals influence the transport of PLP into and/or out of LEs/Ls in oligodendrocytes.

The cholesterol-dependent and clathrin-independent internalization of PLP is reduced after coculturing with neurons

Next, we determined whether endocytosis accounts for the transport of PLP to LEs/Ls and, if so, how its endocytic trafficking is regulated. To block endocytosis, we transiently transfected Oli-neu cells with a mutant form of dynamin-II that is defective in GTP binding (K44A; Damke et al., 1994) and PLP-myc. We found that dynamin-II (K44A) reduced the colocalization of PLP with Lamp-1 and, at the same time, increased the fraction of PLP at the cell surface (Fig. 3), suggesting that endocytosis is required for the transport of PLP to LEs/Ls. A reduction of the intracellular accumulation of PLP was also observed when dynamin K44A was expressed in OLN-93 cells (not depicted).

To gain more insight into the endocytosis process of PLP, the endocytic uptake of PLP was determined by additional antibody uptake experiments using the O10 mAb. To determine whether clathrin function is involved, we either depleted cells of potassium to disrupt the formation of clathrin-coated pits or used the dominant-negative mutant of Eps15 (EΔ95/295; Benmerah et al., 1999). Despite that EΔ95/295 and K$^+$ depletion had no significant effect on the uptake of O10, it led to the reduction of clathrin-mediated transferrin–rhodamine internalization (Fig. 4 a). In addition, intracellular accumulation of PLP was not reduced when EΔ95/295 was coexpressed in OLN-93 (not depicted). Furthermore, we did not detect a significant colocalization of PLP and clathrin on the surface of OLN-93 (colocalization was ~5%; Fig. 4 b) or primary oligodendroglial cells (Fig. S2; available at http://www.jcb.org/cgi/content/full/jcb.200509022/DC1). These results strongly suggest that the internalization of PLP occurs by a clathrin-independent endocytosis pathway.

Most clathrin-independent endocytosis pathways are sensitive to cholesterol depletion or actin depolymerization (Parton and Richards, 2003). Therefore, we used methyl-β-cyclodextrin (mβCD) to selectively extract cholesterol from the cell surface and latrunculin A to prevent actin polymerization. Treatments with either mβCD or latrunculin A led to an almost complete inhibition of O10 uptake (Fig. 4 c). The conditions of the cholesterol depletion experiments were established so that clathrin-dependent endocytosis was not affected as evaluated by the uptake of transferrin–rhodamine. Some clathrin-independent endocytosis pathways require dynamin, whereas others are independent of dynamin function (Lamaze et al., 2001; Pelkmans et al., 2001; Sabharanjak et al., 2002; Damm et al., 2005; Kirkham et al., 2005). The uptake of O10 was clearly reduced by interfering with dynamin function (Fig. 4 d), which is consistent with the redistribution of PLP to the cell surface by dynamin-II (K44A; Fig. 3). Because both cholesterol and dynamin are essential for caveolar-dependent uptake, we compared the localization of PLP to caveolin-1 and GFP-caveolin. Caveolin-1 and GFP-caveolin were detected in punctate arrays on the plasma membrane and on intracellular compartments, but no colocalization with PLP was seen (Fig. S2 and not depicted), suggesting that caveolae are not involved in the endocytosis of PLP. The Rho family of small GTPases differentially regulate nonclathrin and noncaveolar endocytosis pathways. Although cdc42 is involved in the endocytosis of glycosyl-phosphatidyl-inositol–anchored proteins by a pinocytic pathway to recycling endosomes (Sabharanjak et al., 2002), rhoA has been implicated in the dynamin-dependent uptake of interleukin 2 receptor to LEs/Ls (Lamaze et al., 2001). When O10 uptake experiments were performed with dominant-negative mutants of either cdc42 or rhoA, we observed a significant reduction of internalization when the function of rhoA but not cdc42 was inhibited (Fig. 4 d). In summary, our results show that OLN-93 cells use a clathrin-independent but cholesterol-dependent endocytosis pathway that requires a functional actin cytoskeleton and the rhoA GTPase.

To test whether the capacity for endocytosis of PLP changes after contact with neurons, we added OLN-93 cells to neuronal cultures and compared the uptake of O10 into cells that were cultured without neurons. We observed a significant reduction in the internalization of PLP in cells in coculture as compared with cells cultured without neurons (Fig. 4 e). We also analyzed the reduction of cell surface PLP upon various times in culture with or without neurons using the O10 mAb internalization assay. The amount of O10 mAb remaining at the cell surface was analyzed by incubating cells with [^{125}I]-labeled secondary antibody at 4°C. We found that PLP was cleared more efficiently over time from the surface of OLN-93 cells that were cultured without neurons as compared with cells in coculture. Together, these results indicate that neurons reduce the endocytosis of PLP (Fig. 4 f).

Neurons trigger the retrograde transport of PLP from LEs/Ls to the surface of oligodendrocytes

Reduction of endocytosis appears to be one reason why PLP disappears from LEs/Ls after contact with neurons. Another event that could simultaneously contribute is the increased resorting of PLP to the plasma membrane by retrograde transport from LEs/Ls. There are many examples (e.g., wound healing, cytotoxic lymphocyte killing, major histocompatibility complex [MHC]–II processing, and melanin secretion) that show that lysosomes are not merely degradative dead ends but are able to store and release proteins in a regulated fashion (Blott and Griffiths, 2002).

To analyze the putative exocytic trafficking of PLP from LEs/Ls, we performed live cell imaging experiments with
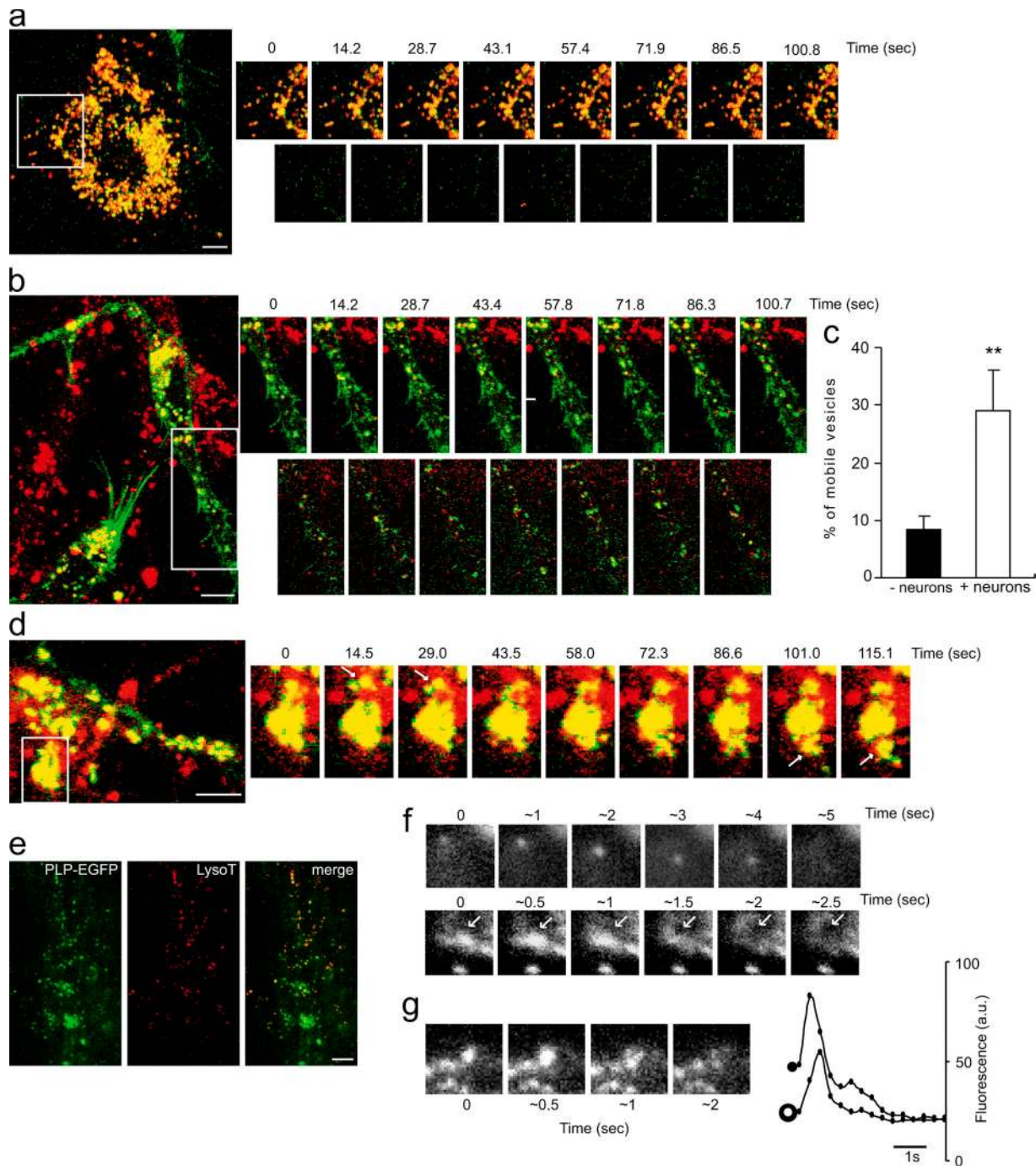
Figure 5. **Neurons trigger the retrograde transport of PLP from LEs/Ls to the surface of oligodendrocytes.** (a) Living PLP-EGFP–expressing Oli-neu cells were labeled with LysoTracker red and observed by confocal microscopy. Images were collected every ∼15 s. The image sequences of the boxed areas (a, b, and d) are shown. Representative examples of a time stack are shown in the top panels. The images in the bottom panels were obtained by subtracting from each image in the top panels. The absence of signal in the subtractions demonstrates the immobility of vesicles. (b) Cells were added onto a neuronal culture and imaged ∼8 h later. The subtractions (bottom) of consecutive frames (top) demonstrate the mobility of PLP and LysoTracker-containing vesicles. (c) The mean fraction of mobile vesicles calculated by the subtraction of consecutive frames (mean ± SD [error bars] of 15 cells; 26 consecutive time frames were analyzed for each cell). **, P < 0.001; t test. (d) Individual frames from a video of a cell prepared as in b. Images were taken every ∼15 s. The frame sequence illustrates the exit (indicated by arrows) of PLP and LysoTracker-containing vesicles from perinuclear LEs/Ls. (e) The TIRFM image demonstrates the colocalization of PLP-EGFP and LysoTracker within 100 nm of the plasma membrane in Oli-neu cells in coculture with neurons. (f and g) Exocytic fusion of vesicles was visualized by time-lapse TIRFM of Oli-neu cells in coculture with neurons. (f) The vesicles that lost their fluorescence during the time of observation fell into two groups. An example of vesicles moving in and out of the evanescent field without fusing is shown in the top panels. Vesicles fusing with the plasma membrane are shown in the bottom panels (indicated by arrows) and in g. Increase in brightness, lateral spread, and disappearance of vesicular fluorescence indicates fusions. (g) The fluorescence intensity changes (in arbitrary units) were determined in a small circle enclosing the vesicle (closed symbol) and in a concentric ring around the circle (open symbol). Other examples of fusions are shown as a flash of fluorescence (LysoTracker channel; Video 3, available at http://www.jcb.org/cgi/content/full/jcb.200509022/DC1). Bars, 5 μm.
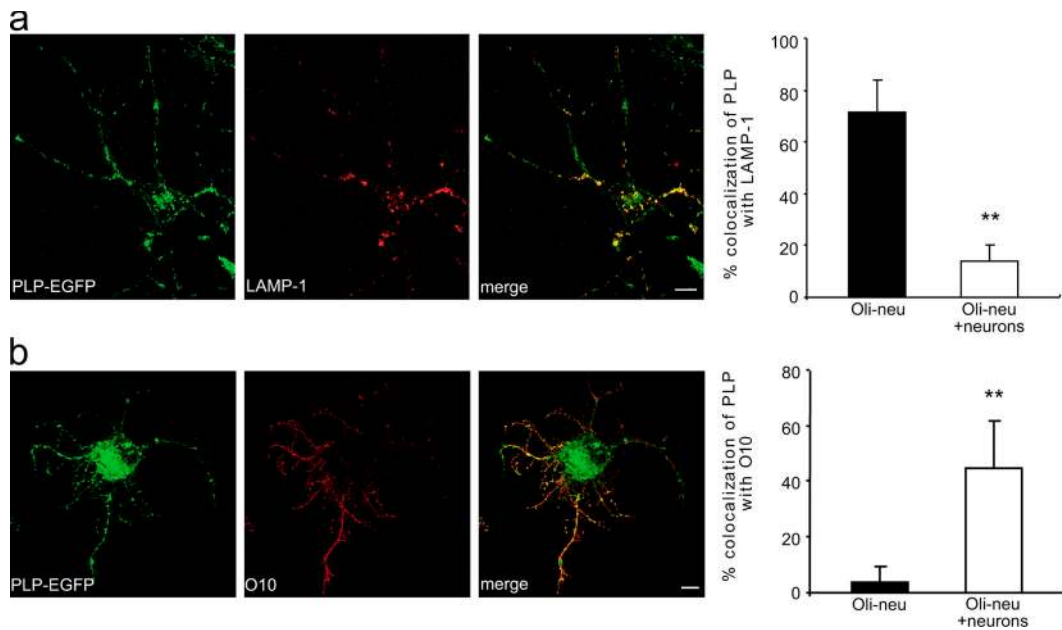
Figure 6. **A soluble factor is sufficient for redistributing PLP from LEs/Ls to the cell surface.** Oli-neu cells expressing PLP-EGFP were added to a neuronal culture on a separate coverslip to prevent cell contact allowing diffusible factors to reach the cells. After 1 d, cells were stained for Lamp-1 (a) or for surface PLP with O10 mAb (b) on living cells at 4°C. Quantitative analysis of the colocalization of PLP-EGFP with Lamp-1 and O10 are shown. Error bars represent SD ($n > 60$ cells). **, $P < 0.001$; t test. Bars, 5 μm.

LysoTracker in PLP-EGFP–expressing Oli-neu cells. There was an almost complete colocalization of PLP-EGFP and LysoTracker (Fig. 5 a) similar to the observation in OLN-93 cells. Analysis of the dynamics of PLP-EGFP/LysoTracker vesicles in Oli-neu cells revealed that most vesicles were clustered perinuclearly and did not show any significant movement (Fig. 5 a and Video 1, available at http://www.jcb.org/cgi/content/full/jcb.200509022/DC1). Next, we investigated whether the movement of the vesicles changes as a result of the presence of neurons. When live cell imaging experiments were performed shortly (6–12 h) after the addition of Oli-neu cells to neuronal cultures, an extensive colocalization of PLP-EGFP and LysoTracker (Fig. 5 b) was still observed. However, the movement of these vesicles was markedly increased. Two pools of vesicles could be distinguished: a perinuclear, immobile pool and a peripheral pool of highly mobile vesicles (Fig. 5 b and Video 2). Both pools of vesicles colocalized with Lamp-1. Quantitative analysis revealed that ∼29% of the vesicles were mobile and exhibited a mean speed of ∼0.56 μm/s (Fig. 5 c). The pool of perinuclear vesicles not only decreased in size (Fig. 2), but the individual vesicles also became smaller with increasing time in coculture (∼33% decrease after 16 h of coculture; reduction from 0.96 ± 0.2 μm to 0.63 ± 0.19 μm; $n = 96$). In several cases, PLP-EGFP and LysoTracker-filled vesicles emanated from larger perinuclear vesicles and moved radially toward the plasma membrane at the cell periphery (Fig. 5 d).

To analyze the behavior of the peripheral vesicle pool, we used total internal reflection fluorescence microscopy (TIRFM). TIRFM allows the selective illumination of a region within a 70–120-nm distance of the plasma membrane as the excitatory evanescent field decays exponentially from the interface of the cell membrane with the coverslip. We observed PLP-EGFP and LysoTracker-containing vesicles within the 100-nm vicinity of the plasma membrane in living Oli-neu cells that were cocultured with neurons (Fig. 5 e). In contrast, no PLP-EGFP and LysoTracker-containing vesicles were observed in the proximity of the plasma membrane when cells were cultured without neurons.

To determine whether the acidic vesicles fuse with the plasma membrane, we used time-lapse TIRFM imaging. The cells we studied contained 6 ± 2.4 vesicles per 100-μm² area of the plasma membrane. The vesicles that lost their fluorescence during the time of observation fell into two groups. We found vesicles moving in and out of the evanescent field without fusing and vesicles fusing with the plasma membrane (Fig. 5 f, top). Fusion was defined by the loss of vesicular fluorescence and the concurrent lateral spread of the released dye into the medium (Fig. 5 g). We detected one to two fusion events/minute per cell at the plasma membrane. When Oli-neu cells were cultured without neurons, we did not observe any fusions in agreement with the absence of PLP-EGFP and LysoTracker-containing vesicles at the plasma membrane.

A cAMP-dependent neuronal signal regulates the trafficking of PLP

Because the redistribution of PLP from LEs/Ls to the surface of the plasma membrane was only observed in Oli-neu cells grown in the presence of neurons, neuronal signals are likely to activate this pathway. We wanted to determine whether this neuronal signaling is transferred as a soluble factor or is a consequence of direct cell-to-cell contact. Oli-neu cells were either directly added on top of a neuronal culture or placed on a separate coverslip to prevent cell contact, allowing diffusible factors to reach the cells. We found that diffusible factors were sufficient to redistribute PLP from LEs/Ls to the surface of the cell (Fig. 6).
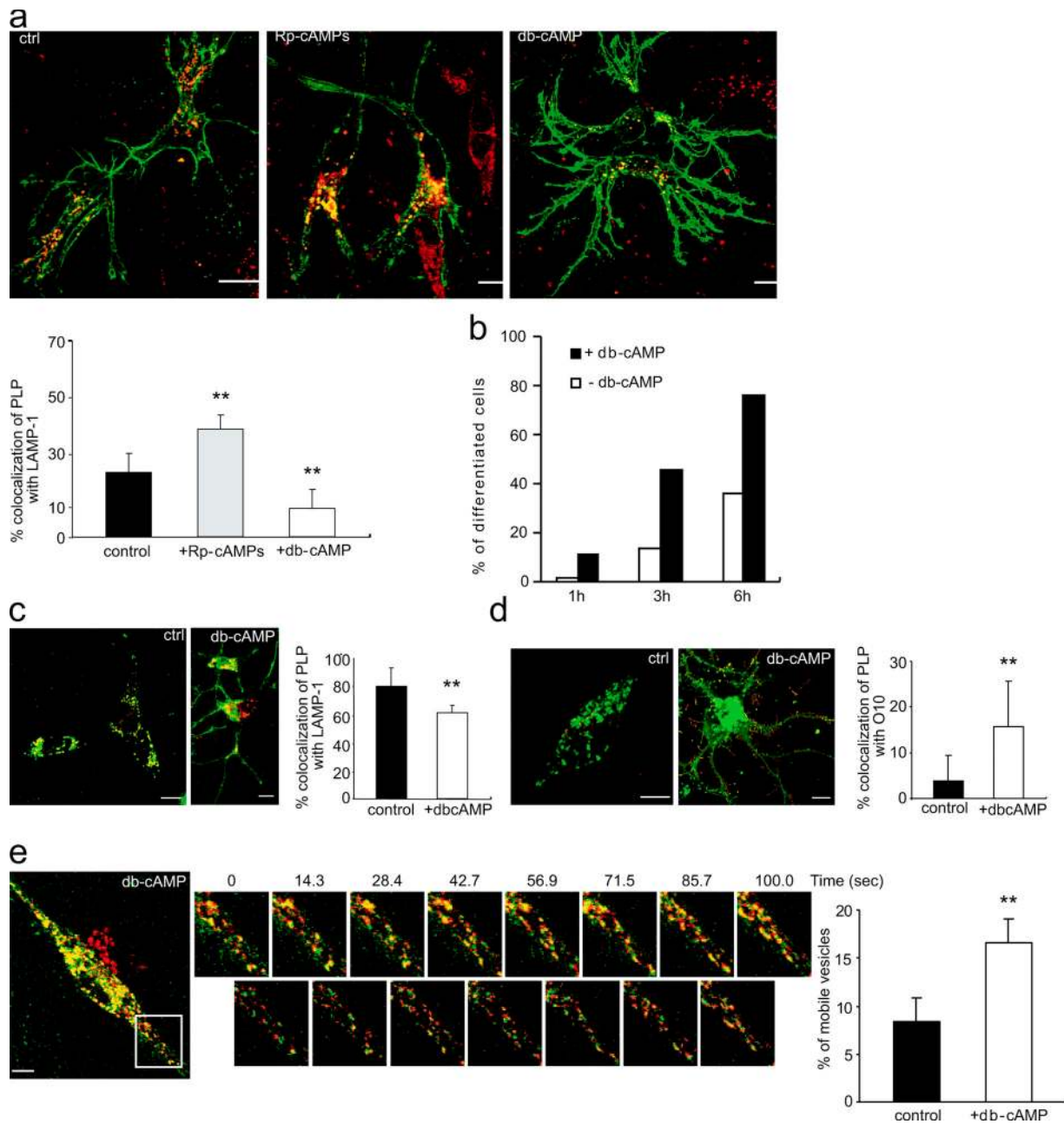
Figure 7. **A cAMP-dependent neuronal signal regulates the release of PLP from LEs/Ls in Oli-neu cells.** (a) Oli-neu cells were cocultured with neurons for 1 d in the presence or absence of 100 µM Rp-cAMPs or 1 mM db-cAMP. Quantitative analysis of the colocalization of PLP-EGFP with Lamp-1 is shown as the mean ± SD of >30 cells. (b) Time-course experiments demonstrate that treatment of Oli-neu cells in the presence of neurons with 1 mM db-cAMP accelerates the removal of PLP-EGFP from Lamp-1–positive compartments. The quantitative analysis of one representative experiment (out of three independent experiments) is shown. Analysis was performed by classifying cells into two categories according to the extent of the colocalization of PLP-EGFP with Lamp-1. (c and d) Oli-neu cells were grown without neurons and treated with 1 mM db-cAMP for 1 d and stained for Lamp-1 (c) or for surface-PLP with O10 mAb (d) on living cells at 4°C. Quantitative analysis of the colocalization of PLP-EGFP with Lamp-1 and O10 are shown. Error bars represent SD (n = 30 cells). (e) Oli-neu cells grown without neurons were treated for 1 d with 1 mM db-cAMP and imaged as in Fig. 5 a. An image sequence of the boxed area is shown. The images in the bottom panels represent subtractions of the consecutive frames in the top panels. The analysis demonstrates a significant increase in the mobility of PLP and LysoTracker-containing vesicles by treatment with db-cAMP as compared with the control condition. **, P < 0.001; t test. Bars, 5 µm.

To analyze the signals involved, we treated Oli-neu cells cultured in the presence of neurons with various pharmacological kinase inhibitors. Colocalization of PLP-EGFP and Lamp-1 increased markedly when cocultures were treated for 1 d with Rp-cAMPs to inhibit protein kinase A (Fig. 7 A). In contrast, treatment of cocultures with db-cAMP, a protein kinase A agonist, promoted the localization of PLP to the plasma membrane (Fig. 7 A). Quantitative analysis of time-course experiments showed that db-cAMP accelerated the redistribution of PLP to the surface of the cell (Fig. 7 B). To test whether similar effects were observed in Oli-neu cells cultured without neurons, we treated Oli-neu cells for 1 d with db-cAMP

and quantified the amount of PLP-EGFP in LEs/Ls and on the surface of the cell. In cells treated with db-cAMP, more PLP was found on the surface of the cell, whereas, at the same time, the fraction within LEs/Ls decreased (Fig. 7, C and D). Furthermore, a peripheral pool of highly mobile PLP-EGFP/ LysoTracker-containing vesicles was observed by live cell imaging (Fig. 7 E). These data suggest that cAMP-dependent signaling is part of the developmental switch that is triggered by neurons, leading to the redistribution of PLP from LEs/Ls to the surface of the plasma membrane.

Discussion

Our data demonstrate that the trafficking of PLP in oligodendrocytes is under neuronal control. PLP is initially targeted to LEs/Ls by using a cholesterol-dependent and clathrin-independent endocytosis pathway. The situation changes dramatically upon receiving maturation signals from neurons. PLP is then redistributed from LEs/Ls to the plasma membrane. We provide evidence that the developmental regulation of PLP localization occurs by the down-regulation of endocytosis and by the transport from LEs/Ls to the cell surface.

The regulation of the transport of PLP is strikingly similar to the trafficking of MHC-II in dendritic cells (Mellman and Steinman, 2001). Immature dendritic cells have a high rate of endocytosis and target MHC-II to lysosomes (Pierre et al., 1997). After exposure to inflammatory mediators, the endocytosis of MHC-II is reduced, and the transport of MHC-II from lysosomes to the cell surface is triggered (Kleijmeer et al., 2001; Boes et al., 2002; Chow et al., 2002). The transport pathway of PLP from LEs/Ls can also be related to the release of secretory lysosomes from hematopoietic cells. However, unlike the classic secretory lysosomes that are specialized to release luminal content, oligodendrocytes mainly transport membrane, and this may occur without significant extracellular release of lysosomal content, as is the case for dendritic cells (Kleijmeer et al., 2001; Trombetta et al., 2003). For oligodendrocytes, LE/L compartments may be particularly useful as storage compartments, as they are able to harbor large amounts of membrane in a multilamellar and multivesicular fashion for myelin biogenesis. In most cells, however, the majority of molecules that localizes to internal vesicles of the endosomal system are destined for lysosomal degradation. This raises the question of how PLP survives in an environment where protein degradation usually occurs. One possibility is that immature oligodendrocytes have specialized LEs/Ls with low proteolytic capacity. Our unpublished observation that the vesicular stomatitis virus glycoprotein accumulates undegraded in LEs/Ls of Oli-neu cells supports this notion. In dendritic cells, for example, lysosomal proteolysis is regulated in a developmentally linked fashion (Trombetta et al., 2003; Delamarre et al., 2005). Another possibility is that PLP is poorly degradable and, therefore, accumulates within LEs/Ls. A second issue is how PLP escapes from a compartment associated with the limited capacity for membrane recycling. Previous work has provided evidence that not all intralumenal membranes of LEs/Ls are destined for lysosomal degradation. It has been suggested that some vesicles may undergo back fusion with the limiting membrane, and, in some instances, this membrane is sorted via tubulovesicles to the plasma membrane (Kleijmeer et al., 2001; Boes et al., 2002; Chow et al., 2002; Abrami et al., 2004; Le Blanc et al., 2005). Whether PLP is sorted by back fusion and tubules to the surface of oligodendrocytes are issues that have to be addressed in future studies. It is important to note that the accumulation of PLP at the surface of the plasma membrane after the receipt of maturation signals most likely reflects the contribution of multiple factors. Our finding that the endocytosis of PLP is reduced after receiving signals from neuronal cells suggests that the regulation of endocytosis may play an essential role in this process. It will be interesting to elucidate the molecular mechanisms of how neurons control the rate of endocytosis in oligodendrocytes. One attractive possibility is that the endocytic activity is controlled by the RhoA GTPase.

Importantly, not all myelin components were found to be internalized into LEs/Ls. Although PLP and cholesterol resided in LEs/Ls, myelin basic protein and galactosylceramide were mainly found in or at the plasma membrane (unpublished data). The differential compartmentalization of myelin components before the onset of myelination might be a mechanism to prevent premature and inappropriate assembly. Our results suggest that an external soluble factor regulates myelin membrane assembly by controlling the trafficking of PLP to and from the surface of the cell. Among the many potential candidates are soluble mediators such as neurotrophins, neuregulin, or adenosine that can now be tested with the described experimental system (Barres and Raff, 1999; Fields and Stevens-Graham, 2002).

Together, our findings reveal an unexpected and novel role of LEs/Ls in oligodendrocytes. It provides a striking example of how cell-to-cell communication regulates trafficking to and from a cellular compartment to guide the development of a multicellular tissue. The proposed role of LEs/Ls in myelin biogenesis may help to explain the cellular mechanisms of dysmyelination that is observed in many lysosomal storage diseases.

Materials and methods

Antibodies, plasmids, and other reagents
The mutant and wild-type cDNAs of GFP-Eps15 and GFP–dynamin-II were provided by A. Benmerah (Institut Pasteur, Paris, France) and S. Schmid (Scripps Research Institute, La Jolla, CA), respectively. The following primary antibodies were used: myelin basic protein (monoclonal IgG; Sternberger, Inc.), PLP (polyclonal, P6; Linington and Waehneldt, 1990), O10 (monoclonal mouse IgM), βIII-tubulin (Promega), neurofilament (monoclonal IgM; Qbiogene), τ (polyclonal; DakoCytomation), myc tag (monoclonal IgG; Cell Signaling), clathrin heavy chain (monoclonal IgG; BD Transduction Laboratories), GFP (Synaptic Systems GmbH), caveolin-1 (monoclonal IgM; BD Biosciences), and Lamp-1 (CD107a, rat monoclonal; BD Biosciences). Secondary antibodies were obtained from Dianova and GE Healthcare.

Cell culture, cloning, and transfections
Primary cultures of mouse oligodendrocytes were prepared as described previously (Simons et al., 2000). After shaking, cells were plated in MEM containing B27 supplement, 1% horse serum, L-thyroxine, tri-iodo-thyronine, glucose, glutamine, gentamycine, pyruvate, and bicarbonate on poly-L-lysine–coated dishes or glass coverslips. Cocultures of neurons and oligodendrocytes were produced by preparing mixed brain cultures from 16-d-old fetal mice that were cultivated for 2 wk, to which the primary oligodendrocytes or Oli-neu cells were added. The mixed brain cultures were

prepared at a density of ∼50,000 cells/cm². Cocultures without direct neuron–glia contact were prepared by growing neuronal cultures on glass coverslips, which were placed upside down on a metal ring positioned in a culture dish. Oligodendrocytes were added on an additional coverslip facing upwards. The oligodendroglial precursor cell line, Oli-neu (provided by J. Trotter, University of Mainz, Mainz, Germany), and OLN-93 cells (provided by C. Richter-Landsberg, University of Oldenburg, Oldenburg, Germany) were cultured as described previously (Jung et al., 1995; Richter-Landsberg and Heinrich, 1996). Transient transfections were performed using FuGENE transfection reagent (Roche) according to the manufacturer's protocol. PLP-EGFP was generated by fusing EGFP to the COOH terminus of PLP by gene fusion PCR. The fusion product was cloned into pEGFPN1 vector using the EcoRI–NotI site. Stable cell lines were obtained by the cotransfection of PLP-EGFPNI and pMSCV-hygro (CLONTECH Laboratories, Inc.) followed by the selection of clones by incubation with hygromycin.

Immunofluorescence and endocytosis assays

Immunofluorescence and immunohistochemistry were performed as described previously (Simons et al., 2002). For assaying endocytosis, living cells were incubated with O10 antibody in medium for 30 min at 4°C, washed, and incubated in medium at 37°C for 60 min. The antibody remaining on the surface was removed under low pH conditions in 0.2 M glycine and 0.5 M NaCl, pH 4.5, for 30 min at 4°C. Cells were washed three times in PBS, fixed, and stained by immunofluorescence. Additionally, OLN-93 cells were transiently transfected with PLP and added on a neuronal culture or left alone. Cells were incubated at 4°C for 30 min with O10 antibody in binding medium consisting of HBSS and 10 mM Hepes supplemented with 0.2% BSA 16 h after transfection. After washing, O10 internalization was allowed to continue for 0, 45, and 90 min. O10 antibody remaining at the cell surface was detected with 5–20 μCi/μg [^{125}I]-labeled mouse secondary antibody in binding medium for 30 min at 4°C. Next, the cells were washed five times, lysed in 0.2 M NaOH, and the amount of radioactivity was determined by γ counting.

Microscopy and analysis

Fluorescence images were acquired on a microscope (DMRXA; Leica) or a confocal microscope (LSM 510; Carl Zeiss MicroImaging, Inc.) with a 63× oil plan-Apochromat objective (NA 1.4; Carl Zeiss MicroImaging, Inc.). For live cell imaging, coverslips containing the cells were mounted in a live cell imaging chamber and observed in low fluorescence imaging medium (HBSS, 10 mM Hepes, and 1% horse serum, pH 7.4) at 37°C. Temperature was controlled by means of a digital system (Tempcontrol 37-2; PeCon) or a custom-built perfusion system. Time-lapse imaging was performed on a confocal laser scanning microscope (LSM 510; Carl Zeiss MicroImaging, Inc.). Images were acquired at ∼15-s intervals for the indicated time periods using sequential line excitation at 488 and 543 nm and appropriate band pass emission filters.

Image processing and analysis were performed using Meta Imaging Series 6.1 software (Universal Imaging Corp.). Quantification of colocalization was performed with the colocalization module of the software. Vesicle movement was analyzed by subtracting from each image in a time stack preceding its image. The different image stack thus generated was used to identify vesicle motility events. The velocity of individual vesicles was determined using the Manual Tracking plug-in for ImageJ software (National Institutes of Health). Statistical differences were determined with a t test. TIRFM was performed on a custom-built prism-based evanescent field microscope using an HCX Apo L 63× water immersion objective (NA 0.90; Leica; Oheim et al., 1998). Evanescent field excitation was obtained by focusing 488- and 568-nm laser light onto a hemicylindrical prism at 68 and 71° incidence angles, respectively, leading to a field depth of ∼80–100 nm. Images were acquired with a back-illuminated 16-bit CCD camera (Cascade 512B; Roper Scientific) with on-chip charge multiplication. Each pixel corresponded to 0.25 μm in the specimen plane. For analysis of individual fusion events, a small circle was positioned on the vesicular fluorescence, a concentric ring was placed around the circle, and fluorescence intensity was plotted against time. Fusion events were identified by the increase of fluorescence in the central region that spread into the surrounding annulus followed by a sudden decline (Schmoranzer et al., 2000; Zenisek et al., 2000; Becherer et al., 2003; Bezzi et al., 2004). Immuno-EM was performed as described previously (Wenzel et al., 2005).

Metabolic labeling and immunoprecipitations

For metabolic labeling, cells were pulsed with 265 μCi [^{35}S]methionine (1 Ci = 37 GBq; GE Healthcare) in methionine and cysteine-free DME for 18 h, and chase was performed for 0 or 48 h. Immunoprecipitation was

performed as described previously (Simons et al., 2000). Autoradiographs were scanned and quantified with ScionImage software (Scion Corp.). Values are shown as means ± SD. Statistical differences were determined with a t test.

Online supplemental material

Fig. S1 shows that EGFP-tagged PLP is sorted to myelin. Fig. S2 shows the absence of PLP colocalization with clathrin heavy chain or caveolin-1. Video 1 shows the movement of LEs/Ls in Oli-neu cells, whereas Video 2 shows this in Oli-neu cells cultured with neurons. Video 3 shows the fusion of vesicles with the plasma membrane. Online supplemental material is available at http://www.jcb.org/cgi/content/full/jcb.200509022/DC1.

References

Abrami, L., M. Lindsay, R.G. Parton, S.H. Leppla, and F.G. van der Goot. 2004. Membrane insertion of anthrax protective antigen and cytoplasmic delivery of lethal factor occur at different stages of the endocytic pathway. *J. Cell Biol.* 166:645–651.

Barres, B.A., and M.C. Raff. 1999. Axonal control of oligodendrocyte development. *J. Cell Biol.* 147:1123–1128.

Baumann, N., and D. Pham-Dinh. 2001. Biology of oligodendrocyte and myelin in the mammalian central nervous system. *Physiol. Rev.* 81:871–927.

Becherer, U., T. Moser, W. Stuhmer, and M. Oheim. 2003. Calcium regulates exocytosis at the level of single vesicles. *Nat. Neurosci.* 6:846–853.

Benmerah, A., M. Bayrou, N. Cerf-Bensussan, and A. Dautry-Varsat. 1999. Inhibition of clathrin-coated pit assembly by an Eps15 mutant. *J. Cell Sci.* 112:1303–1311.

Bezzi, P., V. Gundersen, J.L. Galbete, G. Seifert, C. Steinhauser, E. Pilati, and A. Volterra. 2004. Astrocytes contain a vesicular compartment that is competent for regulated exocytosis of glutamate. *Nat. Neurosci.* 7:613–620.

Blott, E.J., and G.M. Griffiths. 2002. Secretory lysosomes. *Nat. Rev. Mol. Cell Biol.* 3:122–131.

Boes, M., J. Cerny, R. Massol, M. Op den Brouw, T. Kirchhausen, J. Chen, and H.L. Ploegh. 2002. T-cell engagement of dendritic cells rapidly rearranges MHC class II transport. *Nature*. 418:983–988.

Chow, A., D. Toomre, W. Garrett, and I. Mellman. 2002. Dendritic cell maturation triggers retrograde MHC class II transport from lysosomes to the plasma membrane. *Nature*. 418:988–994.

Damke, H., T. Baba, D.E. Warnock, and S.L. Schmid. 1994. Induction of mutant dynamin specifically blocks endocytic coated vesicle formation. *J. Cell Biol.* 127:915–934.

Damm , E.M., L. Pelkmans, J. Kartenbeck, A. Mezzacasa, T. Kurzchalia, and A. Helenius. 2005. Clathrin- and caveolin-1-independent endocytosis: entry of simian virus 40 into cells devoid of caveolae. *J. Cell Biol.* 168:477–488.

Delamarre, L., M. Pack, H. Chang, I. Mellman, and E.S. Trombetta. 2005. Differential lysosomal proteolysis in antigen-presenting cells determines antigen fate. *Science*. 307:1630–1634.

Fields, R.D., and B. Stevens-Graham. 2002. New insights into neuron-glia communication. *Science*. 298:556–562.

Jung, M., E. Kramer, M. Grzenkowski, K. Tang, W. Blakemore, A. Aguzzi, K. Khazaie, K. Chlichlia, G. von Blankenfeld, H. Kettenmann, et al. 1995. Lines of murine oligodendroglial precursor cells immortalized by an activated neu tyrosine kinase show distinct degrees of interaction with axons in vitro and in vivo. *Eur. J. Neurosci.* 7:1245–1265.

Jung, M., I. Sommer, M. Schachner, and K.A. Nave. 1996. Monoclonal antibody O10 defines a conformationally sensitive cell-surface epitope of proteolipid protein (PLP): evidence that PLP misfolding underlies dysmyelination in mutant mice. *J. Neurosci.* 16:7920–7929.

Kirkham, M., A. Fujita, R. Chadda, S.J. Nixon, T.V. Kurzchalia, D.K. Sharma, R.E. Pagano, J.F. Hancock, S. Mayor, and R.G. Parton. 2005. Ultrastructural identification of uncoated caveolin-independent early endocytic vehicles. *J. Cell Biol.* 168:465–476.

Kleijmeer, M., G. Ramm, D. Schuurhuis, J. Griffith, M. Rescigno, P. Ricciardi-Castagnoli, A.Y. Rudensky, F. Ossendorp, C.J. Melief, W. Stoorvogel, and H.J. Geuze. 2001. Reorganization of multivesicular bodies regulates MHC class II antigen presentation by dendritic cells. *J. Cell Biol.* 155:53–63.

Kramer, E.M., A. Schardt, and K.A. Nave. 2001. Membrane traffic in myelinating oligodendrocytes. *Microsc. Res. Tech.* 52:656–671.

Lamaze, C., A. Dujeancourt, T. Baba, C.G. Lo, A. Benmerah, and A. Dautry-Varsat. 2001. Interleukin 2 receptors and detergent-resistant membrane domains define a clathrin-independent endocytic pathway. *Mol. Cell.* 7:661–671.

Le Blanc, I., P.P. Luyet, V. Pons, C. Ferguson, N. Emans, A. Petiot, N. Mayran, N. Demaurex, J. Faure, R. Sadoul, et al. 2005. Endosome-to-cytosol transport of viral nucleocapsids. *Nat. Cell Biol.* 7:653–664.

Linington, C., and T.V. Waehneldt. 1990. Conservation of the carboxyl terminal epitope of myelin proteolipid protein in the tetrapods and lobe-finned fish. *J. Neurochem.* 54:1354–1359.

Mellman, I., and R.M. Steinman. 2001. Dendritic cells: specialized and regulated antigen processing machines. *Cell.* 106:255–258.

Oheim, M., D. Loerke, W. Stuhmer, and R.H. Chow. 1998. The last few milliseconds in the life of a secretory granule. Docking, dynamics and fusion visualized by total internal reflection fluorescence microscopy (TIRFM). *Eur. Biophys. J.* 27:83–98.

Parton, R.G., and A.A. Richards. 2003. Lipid rafts and caveolae as portals for endocytosis: new insights and common mechanisms. *Traffic.* 4:724–738.

Pelkmans, L., J. Kartenbeck, and A. Helenius. 2001. Caveolar endocytosis of simian virus 40 reveals a new two-step vesicular-transport pathway to the ER. *Nat. Cell Biol.* 3:473–483.

Pierre, P., S.J. Turley, E. Gatti, M. Hull, J. Meltzer, A. Mirza, K. Inaba, R.M. Steinman, and I. Mellman. 1997. Developmental regulation of MHC class II transport in mouse dendritic cells. *Nature.* 388:787–792.

Richter-Landsberg, C., and M. Heinrich. 1996. OLN-93: a new permanent oligodendroglia cell line derived from primary rat brain glial cultures. *J. Neurosci. Res.* 45:161–173.

Sabharanjak, S., P. Sharma, R.G. Parton, and S. Mayor. 2002. GPI-anchored proteins are delivered to recycling endosomes via a distinct cdc42-regulated, clathrin-independent pinocytic pathway. *Dev. Cell.* 2:411–423.

Schmoranzer, J., M. Goulian, D. Axelrod, and S.M. Simon. 2000. Imaging constitutive exocytosis with total internal reflection fluorescence microscopy. *J. Cell Biol.* 149:23–32.

Schneider, A., H. Lander, G. Schulz, H. Wolburg, K.A. Nave, J.B. Schulz, and M. Simons. 2005. Palmitoylation is a sorting determinant for transport to the myelin membrane. *J. Cell Sci.* 118:2415–2423.

Simons, M., E.M. Kramer, C. Thiele, W. Stoffel, and J. Trotter. 2000. Assembly of myelin by association of proteolipid protein with cholesterol- and galactosylceramide-rich membrane domains. *J. Cell Biol.* 151:143–154.

Simons, M., E.M. Kramer, P. Macchi, S. Rathke-Hartlieb, J. Trotter, K.A. Nave, and J.B. Schulz. 2002. Overexpression of the myelin proteolipid protein leads to accumulation of cholesterol and proteolipid protein in endosomes/lysosomes: implications for Pelizaeus-Merzbacher disease. *J. Cell Biol.* 157:327–336.

Trombetta, E.S., M. Ebersold, W. Garrett, M. Pypaert, and I. Mellman. 2003. Activation of lysosomal function during dendritic cell maturation. *Science.* 299:1400–1403.

Weimbs, T., and W. Stoffel. 1992. Proteolipid protein (PLP) of CNS myelin: positions of free, disulfide-bonded, and fatty acid thioester-linked cysteine residues and implications for the membrane topology of PLP. *Biochemistry.* 31:12289–12296.

Wenzel, D., G. Schauermann, A. von Lupke, and G. Hinz. 2005. The cargo in vacuolar storage protein transport vesicles is stratified. *Traffic.* 6:45–55.

Zenisek, D., J.A. Steyer, and W. Almers. 2000. Transport, capture and exocytosis of single synaptic vesicles at active zones. *Nature.* 406:849–854.